Materials and Design 200 (2021) 109459

Contents lists available at ScienceDirect

Materials and Design

journal homepage: www.elsevier.com/locate/matdes

Alkyl sulfone bridged phosphorus flame-retardants for polypropylene

Rashid Nazir [a,*], Ali Gooneie [a], Sandro Lehner [a], Milijana Jovic [a], Patrick Rupper [a], Noemie Ott [b], Rudolf Hufenus [a], Sabyasachi Gaan [a,*]

[a] Laboratory of Advanced Fibers, Empa, Swiss Federal Laboratories for Materials Science and Technology, Lerchenfeldstrasse 5, CH-9014 St. Gallen, Switzerland
[b] Laboratory of Joining Technologies and Corrosion, Empa, Swiss Federal Laboratories for Materials Science and Technology, Überlandstrasse 129, CH-8600 Dübendorf, Switzerland

HIGHLIGHTS

- Meltable Alkyl sulfone bridged compounds were synthesized in a simplified method.
- They have thermal stability > 250 °C and melt-processable with polypropylene.
- The incorporation of FR in PP achieves a significant reduction in heat release rates (~48%).
- Incorporation of alkyl sulfone bridged compound improve the thermo-oxidative stability of polypropylene.
- The polypropylene passes vertical burning test with low phosphorus content (1%).

GRAPHICAL ABSTRACT

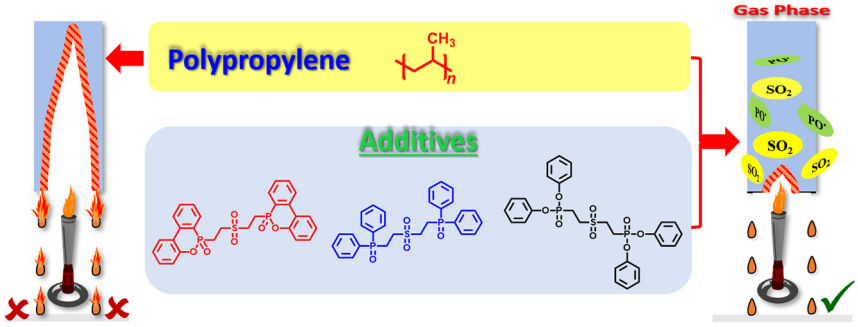

ARTICLE INFO

Article history:
Received 14 October 2020
Received in revised form 5 January 2021
Accepted 7 January 2021
Available online 12 January 2021

Keywords:
Phosphorus
Flame retardant
Bridged sulfone
Sulfur
Alkyl sulfone
Polypropylene
Thermal analysis
Fire tests
LOI

ABSTRACT

Three novel alkyl sulfone bridged phosphorus (P) compounds namely 6,6′-(sulfonylbis(ethane-2,1-diyl))bis(dibenzo[c,e][1,2]oxaphosphinine 6-oxide) (SEDOPO), sulfonylbis(ethane-2,1-diyl))bis(diphenylphosphine oxide) (SEDPPO), and tetraphenyl (sulfonyl bis(ethane-2,1-diyl)) bis(phosphonate) (SEDPP) (i.e. phosphine oxide, phosphinate and phosphonate, respectively) were synthesized via a Michael addition reaction with good yields (≥ 85%) at a 200-g scale. They exhibited thermal stability above 250 °C, which allowed them to be melt-processed with polypropylene (PP) and formed into thin films (~ 0.6 mm). Rheological measurements of the PP blends exhibited a typical shear thinning behavior and provided evidence for the synthesized compound's thermo-oxidative stabilizing effect. This was also confirmed by thermal analysis showing that the thermo-oxidative stability of PP-SEDOPO and PP-SEDPPO blends was higher (~25 °C) than the blank PP; however, PP-SEDPP had a smaller impact. Small scale fire tests of the PP-FR blends confirmed the flame retardant efficacy of the new P-compounds. Cone calorimetry on PP-SEDOPO blends showed a reduction in the heat release rate (HRR) (~48%) compared to blank PP. Further thermal and evolved gas analysis of the PP blends confirmed that the new P-compounds are primarily active in the gas-phase.

1. Introduction

Polypropylene (PP) is a common thermoplastic polymer, which provides a good balance of physical, chemical, mechanical, electrical, and thermal properties with easy processability. This combination of attractive features drives its application in various industries such as electronics, automotive, textiles, construction, and packaging [1–3]. PP is highly

* Corresponding authors.
E-mail addresses: rashid.nazir@empa.ch (R. Nazir), sabyasachi.gaan@empa.ch (S. Gaan).

https://doi.org/10.1016/j.matdes.2021.109459

combustible due to its aliphatic chemical composition [4]. Combustion of PP yields high amounts of toxic gases that threaten human safety and restrict its usage in fire-safe applications [5,6]. A commonly used method to reduce thermoplastic flammability is introducing a flame retardant (FR) additive into the bulk of material via melt processing. Typically, flame retardancy is not the only requirement to be fulfilled by such an FR additive. The FR additive cost of production is a crucial factor for a successful commercial application. Hence, selecting suitable FR additives or the development of new FR systems is a challenging task and mostly depends on the final product specifications and potential fire scenario. Compared to bulk thermoplastic products, flame retardation of fibers and thin films face additional processing and durability challenges [7]. For thin film and fiber applications, the FR additive needs to be either very small in particle size (<1 μm) or in a liquid (meltable) form during its passage through small slits or spinneret holes. The latter type of additive is preferred for fiber applications as non-melting solids tend to agglomerate and clog the spinneret.

The conventional flame-retardants for PP include halogen-based FRs, inorganic FRs, organic halogen-free FRs, phosphorus-containing intumescent FRs (IFR), and metal hydroxide FRs [8,9]. Blends of halogenated compounds with antimony trioxide (Sb_2O_3) can be used as FRs for PP; however, the blend can either produce toxic gases in combustion [10] or are themselves toxic [11]. Inorganic flame retardants such as aluminum hydroxide $Al(OH)_3$ and magnesium hydroxide $(Mg(OH)_2$ are used as FR for PP, but their high loading requirements (~40 wt%) can result in materials with inferior rheological and mechanical properties [12–15] and thus are not suitable for film and fiber fabrication.

N-alkoxy hindered amines (NORs) are commonly used in fiber and thin-film applications [16–20]. They possess excellent flame retardancy due to the dissociation of NORs forming free radical scavengers that interrupt and suppress the ignition process of polyolefins [21,22]. Moreover, NORs can interact with conventional FRs via radical reactions to improve their flame-retardants efficiency and reduce the significant loading of traditional FRs [21,22]. Ciba® FLAMESTAB® NOR® 116 (now BASF) is disclosed in patents as a synergist with conventional brominated and/or phosphorus-based FRs for polyolefins [23,24]. The synergistic effect of FLAMESTAB® NOR 116 [25] in combination with ammonium polyphosphate (APP) and small amounts of nanoclay in PP is also reported [26].

The effectiveness of sulfur(*S*)-containing compounds as FRs has been investigated [27]. They have also been used as co-additives with other FRs, most notably phosphorus compounds, to boost the FR performance of materials [28–35]. Several S-containing compounds have been studied as FRs in polycarbonates (PC) [36], polyamides 6 [37,38], cotton and wool [39], polyurethanes [40], and polystyrene or polymethyl methacrylate [41]. The mechanism for FR of S-containing compounds has been found to vary based on different polymer systems. The thermal decomposition of elemental sulfur, sulfide, and disulfide generates sulfur radicals, which may promote crosslinking at the polymer surface [31,32]. Moreover, S-containing FRs during thermal decomposition generates sulfur dioxide (SO_2) in the gas phase [30], which acts not only as a fuel-diluent, but may also act as a radical-scavenger to suppress combustion efficiency [42,43]. Generally, the flame retardancy of the materials improves as the level of oxygenation at sulfur increases (sulfone > sulfoxide > sulfide) [44]. Thus, a strategy that combines a phosphorus compound with a sulfur moiety for the development of a flame retardant is worthy of investigation. Development of meltable compounds for use as a flame retardant in polyolefins is relatively unknown and will be useful for the advancement of fire safe fibers and films.

In this study, sulfur and phosphorus-based bridged compounds (i.e., phosphine oxide, phosphinate, and phosphonate, Fig. 1) were synthesized by adding P(O)-H containing phosphorus precursors to divinyl sulfone through a straightforward approach. The chemical structure and purity of synthesized FRs were characterized via NMR and elemental analysis. The alkyl sulfone bridged phosphorus derivatives SEDOPO, SEDPPO and SEDPP were processed with PP using extruders and internal mixers and transformed into thin plates (160 × 60 × 0.6 mm) and films (0.6 mm) via compression molding and extrusion, respectively. The PP-FR blends were then analyzed for their thermal, rheological, and flammability properties. Based on the various thermal and evolved gas analysis, a tentative mode of action of the bridged sulfone compounds was proposed.

2. Experimental section

2.1. Materials and methods

9,10-dihydro-9-oxa-10-phosphaphenanthrene-10-oxide (DOPO) was purchased from Metadynea GmbH (Austria), diphenylphosphine oxide (DPPO) was purchased from Combi-Blocks (Germany) and divinyl sulfone was purchased from Fluorochem. Diphenyl phosphonate, 1,8-diazabicyclo(5.4.0)undec-7-ene (DBU) and dry toluene (99.98%) were purchased from Sigma Aldrich (Switzerland) and used without any further purification. The polypropylene (PP) HSP165G (Braskem, The Netherlands) was purchased from Resinex Switzerland AG. 6,6′-(sulfonylbis(ethane-2,1-diyl))bis(dibenzo[c,e] [1,2]oxaphosphinine 6-oxide) (SEDOPO), sulfonylbis(ethane-2,1-diyl))bis(diphenylphosphine oxide) (SEDPPO) [45] and tetraphenyl (sulfonyl bis(ethane-2,1-diyl)) bis(phosphonate) (SEDPP) were synthesized via optimized procedures. The details of optimized procedures and synthesis of FRs are described in the Supporting Information (SI), Sec. SI-1 2.2. Synthesis of bridged sulfone compounds.

2.2. Synthesis of bridged sulfone compounds

2.2.1. 6,6′-(sulfonylbis(ethane-2,1-diyl))bis(dibenzo[c,e][1,2]oxaphosphinine 6-oxide) (SEDOPO)

A dry three-neck, round-bottom flask connected to a mechanical stirrer, nitrogen (N_2) inlet, thermometer, and a condenser was charged with DOPO (187.38 g, 867.5 mmol), divinyl sulfone (50 g, 423.2 mmol), and toluene (600 mL) at room temperature. After the addition was completed, the reaction mixture was heated at 130 °C for 16 h and cooled to

Fig. 1. Structure of alkyl sulfone bridged phosphorus compounds.

room temperature. The reaction mixture was filtered and the solids were washed with acetone and dried at 80 °C overnight under vacuum to obtain a white powder with a 93% yield (Scheme 1).

2.2.2. sulfonylbis(ethane-2,1-diyl))bis(diphenylphosphine oxide) (SEDPPO)

A dry three-neck, round-bottom flask connected to a mechanical stirrer, N_2 inlet, thermometer, and a condenser was charged with diphenylphosphine oxide (DPPO) (82.89 g, 410 mmol), divinyl sulfone (23.63 g, 200 mmol) and toluene (500 mL) at room temperature. After the addition was completed, the reaction mixture was heated to 130 °C for 16 h and then cooled to room temperature. The solid residue was filtered and washed with acetone and dried at 70 °C overnight under vacuum to obtain a white powder with (187 g) 91% yield (Scheme 1).

2.2.3. Tetraphenyl (sulfonyl bis(ethane-2,1-diyl)) bis(phosphonate) (SEDPP)

A dry three-neck, round-bottom flask connected to the mechanical stirrer, N_2 inlet, thermometer, and a condenser was charged with diphenyl phosphonate (203.16 g, 867.5 mmol), divinyl sulfone (50 g, 423.5 mmol) and toluene (1 L) at room temperature. The reaction mixture was cooled to 0 °C and DBU (12.88 g, 84.6 mmol) was added dropwise over 1 h. After the addition of DBU, the reaction mixture stirred for additional 2 h at 0 °C. The solids were filtered and washed with methanol and dried at 60 °C under vacuum overnight to afford 221 g (89%) white powder (Scheme 1).

2.3. Polymer processing

Kneading trials of bridged sulfone compounds were performed by kneading in an internal laboratory mixer (HAAKE Rheomix 600, Thermo Fisher Scientific, Germany) equipped with Banbury type rotor design at a 50 g scale. The blends were prepared in the kneader at 30 rpm for 10 min with a theoretical mass ratio of 90:10 and 85:15 (wt/wt) % of PP: FR additives. A processing temperature of 250 °C for SEDOPO, 220 °C for SEDPPO and SEDPP blends were used for their processing. These PP blends were used to perform thermogravimetric analysis (TGA), differential scanning calorimetry (DSC), and microscale combustion calorimetry (MCC). Moreover, PP plates (160 × 60 × 0.6 mm) were obtained using a compression molding machine Battenfeld Plus 350/75 (Battenfeld Technologies, Columbia, MO, USA), at 250 °C.

Extrusion trials: The main steps for polymer film production included compounding and melt-extrusion of films. First, a 15% masterbatch of SEDOPO in a mixture of PP was prepared by melt extrusion in a co-rotating 36 L/D twin-screw extruder (Dr. Collin GmbH, Germany). To achieve a high SEDOPO loading in the masterbatch, a side feeder (Dr. Collin GmbH, Germany) was used to add the FR powder to the polymer melt. The extruder was operated at 110 rpm with a constant throughput of 0.6–1 kg/h. The extrudate was quenched on a conveyor belt down to room temperature and subsequently pelletized. Second, film extrusion was carried out on a lab-scale extrusion line with a 25 L/D single screw extruder (Rheomex OS, Thermo Fisher Scientific, Germany). FR masterbatch (SEDOPO) pellets were premixed with the blank polymer and fed to the extruder. A static mixer was installed between the extruder and melt pump (Haake OS, Thermo Fisher Scientific) to promote additive dispersion. The extrudate film, pre-shaped by a custom-made 75 mm slit die, was quenched and molded by chill rolls and finally wound up. In both compounding and extrusion processes, the extruder's temperature profile ranged between 240 and 250 °C.

To evaluate the dispersion of FRs in PP, energy dispersive X-ray (EDX) analysis was performed on the sample surface and in cross-sectional view, using a Hitachi S3700N scanning electron microscope (SEM) equipped with an EDAX Octane Pro SDD EDX detector. The SEM device was operated at 7 kV under low vacuum conditions (90 Pa) to avoid beam damage. As shown in Fig. S4, phosphorus and

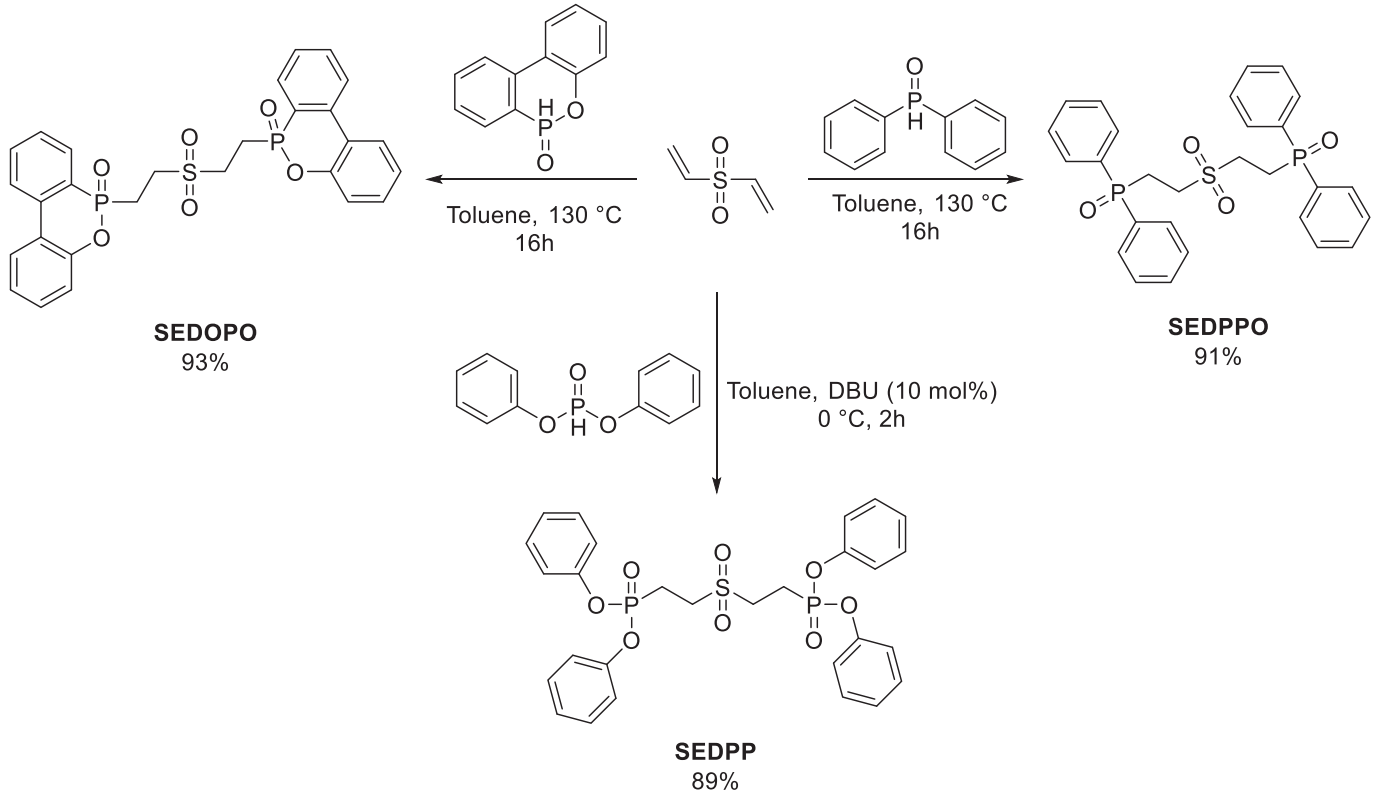

Scheme 1. Synthesis of alkyl sulfone bridged phosphorus compounds SEDOPO, SEDPPO, and SEDPP.

sulfur are present everywhere in the 15% PP-SEDOPO (surface and bulk material showed in cross-sections) films. While the SEDOPO is relatively homogeneously distributed over the cross-section, areas with slightly increased P and S concentrations are found at the surface. Point analysis at different positions confirmed the FR distribution over the whole sample.

2.4. Characterization

NMR spectra were recorded on a Bruker AV-III 400 NMR spectrometer (Bruker Biospin AG, Fällanden, Switzerland) at 298 K. The spectral data and further details about NMR analysis are available in SI part sec. SI-2. NMR characterizations.

Phosphorus content of the PPs blends was measured with a 5110 inductively coupled plasma optical emission spectrometer (ICPOES, Agilent Switzerland AG, Basel, Switzerland). Sample preparation for ICP-OES consisted of mixing 200 mg of a sample with 3 mL HNO_3, followed by microwave digestion.

Differential scanning calorimetry (DSC): For DSC analysis, NETZSCH DSC Polyma 214 was used to analyze the additives melting point and glass transition temperature (T_g) of the PP matrix. For DSC experiments, ca. 5–8 mg of samples were used in a low-pressure crucible and heated to 300 °C at a heating rate of 10 °C/min.

The thermogravimetric analysis (TGA) of the PP samples and synthesized FRs was carried out using a NETZSCH TG209 F1 Iris instrument. For TGA experiments, ca. 3-5 mg of samples were heated from 25 °C to 800 °C at a heating rate of 10 °C/min. The measurements were performed under a nitrogen and air atmosphere with a total gas flow of 50 mL/min.

Limiting Oxygen Index (LOI) values of all plates were measured on an FTT oxygen index apparatus according to ASTM D2863–97. The dimension of specimens for the LOI test was 150 × 50 × 0.5 mm and the samples (plates) were prepared via compression molding.

Vertical burning tests (small scale fire tests) were performed according to the Swiss Standard (BKZ-VB) as described in the literature [46]. PP plates in a vertical orientation were exposed to a flame (45°) for 15 s and the burn length and burn time were measured. Most thermoplastic materials drip when exposed to fire and adequate heat. Thus, in the vertical burning tests, the dripping behavior of the specimens was also observed. The dimension of the specimen for the Vertical burning tests was 160 × 60 × 0.6 mm and the sample was prepared via compression molding.

Direct insertion probe mass spectrometry (DIP-MS) was performed in a Finnigan/Thermoquest GCQ ion trap mass spectrometer (Austin, TX, USA) equipped with a DIP module. ~1 mg of sample was placed in a quartz cup located at the tip of the probe and was inserted into the ionization chamber operating at an ionization voltage of 70 eV, a temperature of the ionic source of 200 °C and pressure $< 10^{-6}$ mbar. The probe was heated from 30 to 450 °C at 50 °C/min.

TGA-FTIR was performed using around ca.10 mg of the samples and heated from 25 to 800 °C at a rate of 10 °C/min^{-1} under a nitrogen purge at 300 mL min^{-1}. The FTIR (Fourier transform infrared spectroscopy) extracted spectra of the pyrolysis gases formed from the samples were measured by Bruker Tensor 27 Fourier transform spectrophotometer coupled with a TGA. The FTIR analysis was performed in the spectral range of 4000 to 550 cm^{-1} at a resolution of 4 cm^{-1}.

Microscale Combustion Calorimeter (MCC) Heat release rates (HRR) were determined using MCC (Fire Testing Technology Instrument, London, UK) following ASTM D7309. ~7 mg of sample was exposed to a heating rate of 1.0 °C/s from 150 to 750 °C in the pyrolysis zone.

Cone calorimetry (Fire Testing Technology, East Grinstead, London, UK) was performed with an irradiative heat flux of 35 kW/m^2 (ISO 5660 standard) on specimens (100 × 100 × 3 mm^3) placed horizontally without any grids. Parameters such as heat release rate (HRR), peak of heat release rate (pHRR), total heat release (THR), total smoke release (TSR), CO production (COP), average specific extinction area (av-SEA), and CO_2 output (CO_2) were recorded for each sample. The cone calorimetry samples were prepared via compression molding.

Activation energy (Ea): Variation in Ea with the degree of conversion for blank PP and PP-15% SEDOPO, SEDPPO, and SEDPP blends were calculated using the Kissinger method using NETZSCH Kinetics Neo software, version 2.4.6 [47]. For the kinetics experiment, 4 different heating rates (i.e., 2.5, 5, 7.5, and 10 °C /min) were used where samples were heated from 25 °C to 800 °C under air atmosphere with a total gas flow of 50 mL/min.

Rheological measurements were carried out on an Anton Paar Physica 301 MCR rotational rheometer (Austria). All experiments were performed at a constant temperature of 250 °C in the air using a parallel plate fixture (plate diameter of 25 mm and 1 mm gap). Samples were compression molded into plates using a hot press at 250 °C. Before starting a measurement, the samples were relaxed for 5 min in the rheometer to minimize the deformation history and get a homogeneous melt. Afterward, angular frequency sweep experiments were conducted at a constant strain of 1%.

Tensile test: The load-strain behavior of dogbone film specimens (Fig. S5) cut in film production direction was evaluated using the Zwick Z100 (Zwick Roell GmbH, Germany) tensile testing machine, equipped with a 100 N load cell. The tensile tests were performed at 23 °C and 50% relative humidity, with an initial gauge length of 50 mm and a constant elongation rate of 20 mm/min. The starting length of the neck was 25 mm, which was considered a reference length for assessing strain. Stress was calculated by dividing the measured load by the initial cross-section area, i.e., the film thickness multiplied with the neck's width (4 mm). The sample used for the tensile test was the film (0.6 mm) obtained via slit extrusion.

3. Results and discussion

3.1. Synthesis of flame retardants and analysis

The addition of the P(O)-H bond to an alkene is a vital transformation for the preparation of organophosphorus compounds with P—C bonds. This addition is often promoted by bases, radical initiators (benzoyl peroxide, AIBN), transition metals, and microwaves [45,48–51]. FR additives consisting of two moieties based on sulfur dioxide and phosphorus were synthesized in this study via the addition of P(O)-H containing precursors to divinyl sulfone. The synthesis of SEDOPO and SEDPPO has been reported in the literature before, but the previous methodology was not feasible for industrial scale-up [45]. The synthesis of 1,2-bisphosphorylethane compounds using toxic trimethylphosphine as a catalyst is previously reported [48]. SEDPPO has been synthesized in solvent-free conditions in an alternative synthesis strategy by reacting one equivalent of divinyl sulfone and two equivalents of diphenylphosphine oxide using a microwave-assisted double-hydrophosphorylation of alkenes on a 50 mg scale [45]. The preparation of a phenylphosphine oxide-bridged phosphorus compound from diethylphosphonic acid using a phosphine catalyzed synthesis is also reported in the literature [52]. With a view to industrial-scale production, the use of alkyl phosphine catalysts is highly undesirable considering their toxicity and potential fire hazard. On the other hand, the microwave heating of a solvent free reaction mixture is challenging, particularly when applied to a high-temperature melting reaction mixture. Accordingly, there is a need for an improved approach to preparing bridged phosphorus-based compounds as these compounds were never tested as flame retardants previously.

The addition of DOPO (1) to divinyl sulfone was chosen as a model reaction and detailed procedures of various reaction conditions are described in SI-1. By following the optimized reaction conditions (method 3, Table S1), SEDOPO and SEDPPO were further synthesized at ~200 g scale with high yields (93% and 91%, respectively) (Scheme 1). Surprisingly, diphenyl phosphite reaction with divinyl sulfone and toluene as a solvent at reflux condition yielded no final product (SEDPP). However, when a catalytic amount of DBU (10 mol%) was added to the reaction

mixture at 0 °C, the desired addition product (SEDPP) was obtained at 89% yield (Scheme 1).

3.2. Thermal processing and rheological behavior

A practical approach to preserving the desired mechanical and thermal properties of PP is to develop a blend with a minimum loading of the FR additive. Usually, a meltable additive can exhibit higher compatibility with PP as compared to non-meltable additives. To evaluate the effect of the bridged sulfone compound on the properties of PP, compounded blends were obtained in the kneader with a theoretical loading mass ratio of 90:10 and 85:15 (wt/wt) % of PP: additives. In general, the effectiveness of a phosphorus-based FR additive relies on phosphorus concentration in the blend. Therefore, it should be noted that the measured phosphorus content in the PP blends containing SEDOPO and SEDPPO additives are very close to the theoretical predictions (Table 1). In contrast, the phosphorus content is almost 40% lower than the theoretical concentration in PP-SEDPP blends. This difference in the phosphorus content of PP-SEDPP blends could be due to polymer and additive's poor compatibility. Being polar (presence of P-O-C bond), SEDPP demixes and separates from PP during the kneading process (Table 1), which results in lower phosphorus contents.

Moreover, it is critical to understand the effects of FR additive on the rheological behavior of the polymer and on its melt stability. The complex viscosity of different PP blends with frequency sweep rheological experiments were characterized and are presented in Fig. 2a, b. Before kneading, the blank PP sample shows a typical Newtonian viscosity at low frequencies followed by a typical shear thinning behavior at higher frequencies. After PP extruded under the conditions explained before, its viscosity reduced, indicating a loss of molecular weight due to thermomechanical degradation. The presence of SEDOPO in PP prevents its degradation; hence, a higher viscosity for the blend is achieved, Fig. 2a. Similar behavior was also observed for PP blends containing other bridged sulfone compounds (SEDPPO and SEDPP) with some differences in effectiveness, Fig. 2b. It has been shown in earlier studies that this protection mechanism of phosphorous additives arises due to a combination of (i) molecular lubrication that reduces stress on polymer chains and (ii) released phosphorous radicals that prevent oxidative attacks on polymer [46,53].

3.3. Small scale fire tests

PP films and fibers need to be fire-resistant in specific applications, for instance, electronics, transportation, and textiles. PP-FR blends were fabricated into plates (0.6 mm thickness) resembling textile fabrics and evaluated for their flammability via a small-scale vertical fire test (BKZ-VB) and limiting oxygen index (LOI) (Table 1). [54,55]. Videos of vertical burning tests and digital photos of residues after burning (Fig. S6) test for blank PP and PP-FR blends are available in SI for blank PP, PP-10% SEDOPO, PP-15% SEDOPO, PP-10% SEDPPO, PP-15% SEDPPO, PP-10% SEDPP and PP-15% SEDPP. The blank PP burned readily without leaving any char in the vertical burning test, as shown in Fig. S6. However, on incorporating bridged sulfone derivatives in PP, a decline in the burning length of PP was observed compared to the blank PP (Fig. S6). No further ignition was observed for the plates containing 10 or 15% SEDOPO after removing the flame, which confirms their self-extinguishing behavior. An increased concentration of bridged sulfone compounds in PP reduced the burning length and duration of the burning. Not much char was formed for the samples in the vertical burning test; it is more likely that the bridged sulfone derivatives primarily work in the gas phase. Furthermore, the PP blends with10% or above loading exhibited no or few drips than the blank PP. The melt dripping was suppressed completely for PP samples containing a minimum of 10% SEDOPO and 15% for other bridged sulfone compounds. PP blends containing 5% bridged sulfone compounds were also manufactured; however, they didn't pass the BKZ-VB test and thus were omitted from any further analytics.

The limiting oxygen index (LOI) value for the blank PP plate is 19.4% [56]; however, the LOI values for various PP blends in this work were significantly higher than the blank PP. Increased LOI values were observed for increased concentration of bridged sulfone compound in PP and the highest LOI was observed for PP containing 15% SEDOPO. As discussed earlier, it is likely that all bridged sulfone compounds work primarily in the gas phase as mostly gas-phase active FRs have a superior influence on promoting the LOI values of polymeric materials.

3.4. Flammability: Pyrolysis combustion flow calorimetry (MCC) measurements

MCC was employed to understand the combustion behavior of the PP blends (Table 2). Fig. S7 illustrates the heat release rate (HRR) profile versus temperature for the blank PP and PP blends. For the blank PP, a peak heat release rate (pHRR) of 1120 $W \cdot g^{-1}$ at 484 °C and a THR of about 45.33 $kJ \cdot g^{-1}$ was observed. The addition of SEDOPO to PP decreased the pHRR by 21% and 27% for 10 and 15% of SEDOPO, respectively. Similarly, a 21% and 25% decline in pHRR was observed for 10 and 15% loadings of SEDPPO in PP, respectively. Furthermore, for 10% loadings of SEDPP in the PP matrix, pHRR (1070 W g^{-1}) values decreased by ~4.5%; THR (46.3 kJ g^{-1}) values were higher than the corresponding blank PP data. For 15% loading of SEDPP in PP, a small decrease in the pHRR of 3.4% and THR around 2.9% was observed. Blank PP and the PP-SEDPP blends were characterized by a one-step thermal decomposition in MCC data. In contrast, a shoulder noticeable for the PP-SEDOPO and PP-SEDPPO blends at 350 °C to 370 °C can be ascribed to the bridged sulfone derivatives that are released due to thermal decomposition and volatilization. A similar observation for the same blends was also made in the TGA analysis performed under an N_2 environment (Fig. S10).

In general, a decrease of the pHRR values corresponds to a drop in the heat produced during the combustion of the flame retarded polymeric material. A reduction in the pHRR and an increase in char formation is often associated with condensed phase activity of the FR additive. In such a case, the FR additive reacts with the polymer matrix and decreases flammable volatiles' formation. However, for PP-SEDOPO,

Table 1
Summary of small-scale fire tests and the limiting oxygen index (LOI).

Samples	Predicted P. [wt%]	Measured P. [wt%]	BKZ-VB[a] Test			LOI % ± 0.2
			After Flame(*sec*) ± 1	Burning Length(cm) ± 1	Melt Drips	
PP-Blank	–	–	40	15	Many	19.4
PP-10% SEDOPO	1.12	1.10	0	2.0	No	24.3
PP-15% SEDOPO	1.69	1.54	0	1.4	No	25.7
PP-10% SEDPPO	1.18	1.09	0	4.6	Few	22.7
PP-15% SEDPPO	1.78	1.54	0	4.2	No	23.5
PP-10% SEDPP	1.05	0.63	3.5	7.0	Many	22.4
PP-15% SEDPP	1.59	0.90	3	6.2	Few	24.9

[a] Swiss standard vertical fire test.

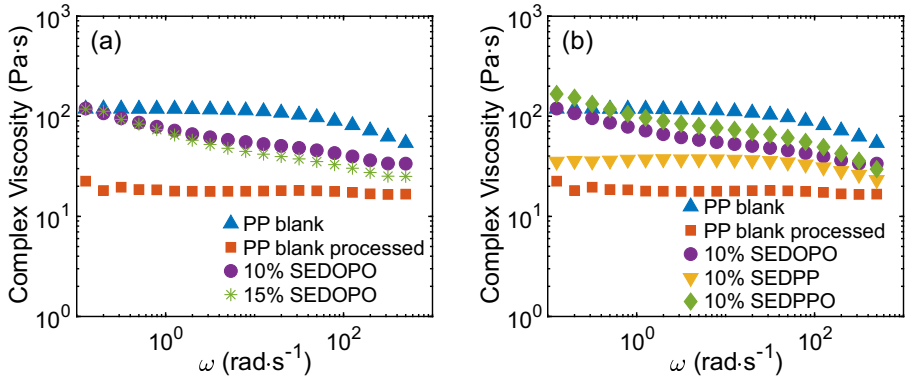

Fig. 2. Rheological behavior of melts at 250 °C in air.

Table 2
Results from MCC measurements.

Sample Name	T_M [°C]	pHRR [W.g^{-1}]	THR [kJ.g^{-1}]	Residue [wt%]
PP-Blank	484.0 ± 0.4	1120.3 ± 16.4	45.3 ± 0.2	0.42 ± 0.30
PP-10% SEDOPO	483.5 ± 0.6	890.7 ± 7.9	43.2 ± 0.4	0.87 ± 0.11
PP-15% SEDOPO	483.4 ± 1.2	809.4 ± 13.9	42.9 ± 0.4	0.26 ± 0.01
PP-10% SEDPPO	482.8 ± 1.3	884.7 ± 12.3	43.7 ± 0.3	0.15 ± 0.1
PP-15% SEDPPO	480.0 ± 1.7	838.0 ± 22.8	43.0 ± 0.2	0.38 ± 0.3
PP-10% SEDPP	491.0 ± 1.3	1070.3 ± 13.8	46.3 ± 2.5	0.32 ± 0.31
PP-15% SEDPP	489.0 ± 1.5	1082.0 ± 39.6	44.0 ± 0.3	0.41 ± 0.3

PP-SEDPPO, and PP-SEDPP blends, a decrease in pHRR with no significant increase in the residue was observed. This corresponds well with the gas phase flame inhibition activity of the FR additive [30,57].

The PP-SEDOPO and SEDPPO blends were characterized by a decrease in THR of approx. 2–3 k·Jg^{-1} relative to the blank PP (Table 2). However, a reduction in the THR is not significant for SEDPP, which might be due to the lower loading and FR efficacy of the SEDPP. A decrease in THR values for the PP blends than blank PP reduces its flame spread and fire load [30].

It is well known that phosphorus content is an important factor in determining the flame retardant efficiency of a system. As seen in Table 1, the P-contents of the 10, 15% SEDOPO (measured P-contents of 1.10, 1.54%), and for the 10, 15% SEDPPO (measured P-contents of 1.09, 1.54%) blends are nearly double compared to the 10, 15% SEDPP blends (measured P-contents of 0.63, 0.90%). The pHRR data of PP-10% SEDOPO and SEDPPO can be compared with the PP-15% SEDPP blends as they have similar P content. The SEDOPO and SEDPPO blends have higher flame retardant efficacy compared to SEDPP at similar P-contents.

3.5. Cone calorimeter test

The cone calorimeter was used to investigate alkyl bridged sulfone derivatives combustion behaviors in the PP matrix. Parameters such as pHRR, THR, TSR, COP, av-SEA, and CO_2 output (CO_2) are summarized in Table 3. Generally, these parameters are used to calculate the fire performance of PP blends. The HRR, particularly the pHRR, represents the point at which fire typically spreads further or ignites neighboring objects; hence, its drop is essential for fire safety. It can be seen from Table 3 that the bridged sulfone/PP blends resulted in a reduction of THR and pHRR; however, TSR and CO production increased, which is typical of flame retardant polymers (Fig. 3). Thus, it is clear from the results that sulfone bridged phosphorus flame-retardants undermine the combustion behavior of PP. All PP blends have a higher CO/CO_2 ratio than the blank PP, indicating their possible gas phase flame inhibition activity. The PP-15% SEDOPO blend has the highest CO/CO_2 ratio and the lowest PHRR compared to PP-15% SEDPPO and SEDPP systems. This indicates a higher gas-phase flame inhibition efficacy of the SEDOPO over SEDPP.

To investigate the gas phase activity of alkyl bridged sulfone derivatives, the combustion efficiency (X) of PP blends was calculated (Table 4). The combustion efficiency can be calculated from the ratio between effective heat of combustion (EHC) measured from cone calorimeter and heat of complete combustion (HCC) calculated from MCC (using THR and residue content) as described in the literature [58]. As shown in Table 4, the EHC of samples containing SEDOPO and SEDPPO decreased significantly compared to SEDPP and blank PP. The combustion efficiency value of all PP blends was lower than the blank PP, indicating a flame inhibition activity of the FRs [59].

3.6. Thermal stability

Understanding the thermal behavior of synthesized bridged sulfone compounds may help predict and understand their subsequent thermal processing, thermal, and fire behavior. The melting point (m.p.) of the bridged sulfone compounds were estimated by DSC (Fig. S8 in SI-5). All synthesized compounds have m.p. ranging from 148 to 248 °C and they are thermally stable up to 321 °C as seen in their TGA data (Table 5). Similarly, bridged DOPO compounds have been shown to exhibit m.p greater than 250 °C [60,61]. The low m.p. exhibited by compounds synthesized in this work allow for melt processing of their blends. Incorporating the bridged sulfone compounds into PP has negligible influence on melting point (Table 5) of PP. TGA evaluated the

Table 3
Results for blank PP and PP-FR (15%) blends obtained from cone calorimeter.

Sample	pHRR (kW/m^2)	THR (MJ/m^2)	TSR (m^2/m^2)	SEA (m^2/kg)	MARHE (kW/m^2)	mean CoP (kg/kg)	mean CO_2 (kg/kg)	CO/ CO_2
PP-Blank	469.5 ± 13.8	62.6 ± 2.0	62.6 ± 20.7	172.86 ± 52	175.3 ± 1.8	0.04 ± 0.01	1.41 ± 0.20	0.03
SEDOPO	241.5 ± 2 4.2	40.0 ± 12.8	941.2 ± 16.9	462.15 ± 15	132.9 ± 7.8	0.15 ± 0.02	0.98 ± 0.02	0.15
SEDPPO	336.2 ± 24.5	46.9 ± 3.6	843.3 ± 15.8	422.4 ± 31	131.6 ± 1.9	0.04 ± 0.02	0.68 ± 0.40	0.06
SEDPP	452.3 ± 7 0.8	67.0 ± 2.7	852.9 ± 16.7	400.4 ± 58	182.0 ± 6.6	0.05 ± 0.01	1.49 ± 0.21	0.04

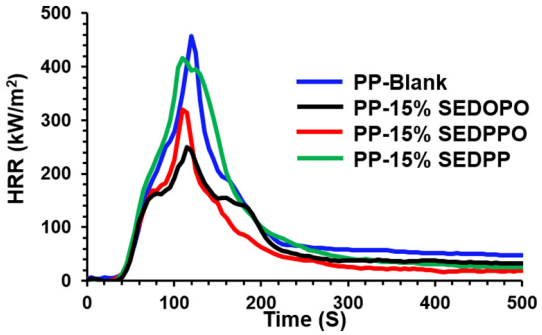

Fig. 3. Heat release rate (HRR) of the blank PP and PP/FRs measured by cone calorimeter.

Table 4
Determination of combustion efficiency (X) from cone calorimeter (CC) and MCC data.

Sample	EHC_{CC} (Kg/g)	HCC_{MCC} (Kg/g)	X
PP-Blank	50.3	78.1	0.64
PP-15% SEDOPO	24.2	57.9	0.41
PP-15% SEDPPO	36.5	69.3	0.52
PP-15% SEDPP	46.6	74.5	0.62

EHC_{CC}: effective heat of combustion, HCC_{MCC}: the heat of complete combustion, X: combustion efficiency (ratio between EHC and HCC).

thermal decomposition behavior of the synthesized compounds and the PP blends. Their corresponding first order derivative (DTG) curves under both air and nitrogen environments are presented in Fig. S9b, d and f, respectively. The TGA data corresponding to the onset of weight loss (T_{donset}), the maximum decomposition rate (T_{dmax}), and the char yield at 800 °C are summarized in Table 5. As shown in Fig. S9, bridged sulfone compounds exhibited high decomposition temperatures (T_{donset} > 290 °C). Among the synthesized bridged sulfone compounds, SEDOPO (T_{donset} ~ 321 °C) showed the highest thermal stability, followed by SEDPP (T_{donset} ~ 317 °C) and SEDPPO (T_{donset} ~ 298 °C) under air atmosphere. The high decomposition temperatures of the compound indicate their suitability for the PP extrusion process, which is usually performed below 250 °C. SEDOPO and SEDPPO decompose completely, leaving residue less than 2% at 800 °C; thus, likely, these compounds may primarily be active in the gas phase. In contrast, SEDPP yields a slightly higher residue of around 6% under the air atmosphere and 18.5% in the N_2 environment at 800 °C.

In general, for all PP blends, higher thermo-oxidative stability was observed compared to blank PP. For PP-SEDOPO, SEDPPO blends, the T_{donset} and T_{dmax} shifted towards higher temperatures in an oxidative environment than blank PP (Table 5). A shoulder is visible in the DTG curve measured under the nitrogen environment for PP-SEDOPO and PP-SEDPPO blends (Fig. S9b, d), indicating the possible early decomposition of SEDOPO and SEDPPO to release volatiles and subsequent decay of PP. Furthermore, a small shift in the thermal stability of PP in both inert and oxidative environments was noted with the incorporation of SEDPP into the PP matrix (Fig. S9e, f). To further understand the thermo-oxidative stability of the bridged sulfone/PP blends, thermal decomposition kinetics experiments were performed (Fig. 4) and activation energy of decomposition was evaluated. The variation in activation energy (E_a) with the degree of conversion for PP and PP-15% SEDOPO, SEDPPO, and SEDPP blends are presented in Fig. 4. The activation energy required to initiate the decomposition ($\alpha = 0$) of PP-SEDPP is 92 kJ.mol^{-1}and, relatively higher than the energy needed to initiate decomposition of PP-SEDOPO and PP-SEDPPO. At the initial stage of conversion ($\alpha = 0.1$), the activation energies for PP, PP-SEDOPO, PP-SEDPPO, and PP-SEDPP are 78, 67, 62, and 62 kJ.mol^{-1}, respectively. For the PP-SEDOPO blend, the activation energy from 80 ($\alpha = 0$) to 109 kJ.mol^{-1} ($\alpha = 0.8$) progresses through different conversion phases. There is a sharp rise in activation energy during the initial stages ($\alpha > 0.1$) of thermal decomposition, representing a decomposition mechanism where SEDOPO strongly interfered in the thermal decomposition process of PP and retard the release of volatiles. Furthermore, the increase in the activation energy of PP-SEDPP at the latter stages of conversion can be due to the limited char formation. This char acts as a thermal barrier and requires higher energy for decomposition. The activation energy for PP, PP-SEDOPO, PP-SEDPPO, and PP-SEDPP at the final stage of decomposition (i.e., $\alpha = 0.8$) are 69, 109, 91, and 112 kJ.mol^{-1}, respectively. Hence, the added FRs in the PP matrix delayed the decomposition of PP. Studies on other FRs in PP have also demonstrated an increase in activation energy of decomposition for PP [62].

The tertiary proton in PP is liable to the free radical degradation mechanism [63,64]. As illustrated in Scheme S1, after removing the tertiary hydrogen, the carbon radicals are liable to react with oxygen (O_2), forming peroxide radicals. The subsequent decomposition of the peroxy radicals follows two possible mechanisms. The first possible degradation mechanism is a termination reaction, leading to a terminal aldehyde or unsaturated group in the case of primary and secondary peroxide radicals.

The second possibility is creating PP polymer chains with a reduced molecular weight by rearrangements at the tertiary carbon radical [65]. Thus, it is essential to have antioxidants or additives which can neutralize polymeric radicals and prevent oxidative degradation [66]. During melt processing at high temperatures, the alkyl sulfone bridged phosphorus compounds (SEDOPO, SEDPPO, and SEDPP) decompose to produce phosphorus and sulfone-based radicals. These radicals react with

Table 5
Thermal properties of blank PP, FR additives, and the PP-FR blends.

Samples	T_{donset} [°C]		T_{dmax} [°C]		Residue at 800 °C [wt%]		Melting Point [°C]	Crystallization Point [°C]
	N_2	Air	N_2	Air	N_2	Air		
PP-Blank	402	241	438	281	0.30	0.61	165	112
SEDOPO	322	321	338	336	4.29	2.67	248	211
PP-10% SEDOPO	412	248	445	294	0.59	1.80	165	118
PP-15% SEDOPO	400	265	444	333	0.59	2.21	166	119
SEDPPO	294	298	309	314	2.20	1.25	202	131
PP-10% SEDPPO	407	250	436	309	1.55	0.30	167	118
PP-15% SEDPPO	406	265	437	314	0.30	1.5	167	115
SEDPP	327	317	341	338	18.5	5.96	148	80
PP-10% SEDPP	418	240	445	288	0.50	1.31	167	116
PP-15% SEDPP	427	246	450	294	0.18	1.23	166	118

T_{donset} (°C): the temperature of weight loss begins and T_{dmax} (°C): the temperature of the maximum mass loss rate measured as the DTG peak maximum.

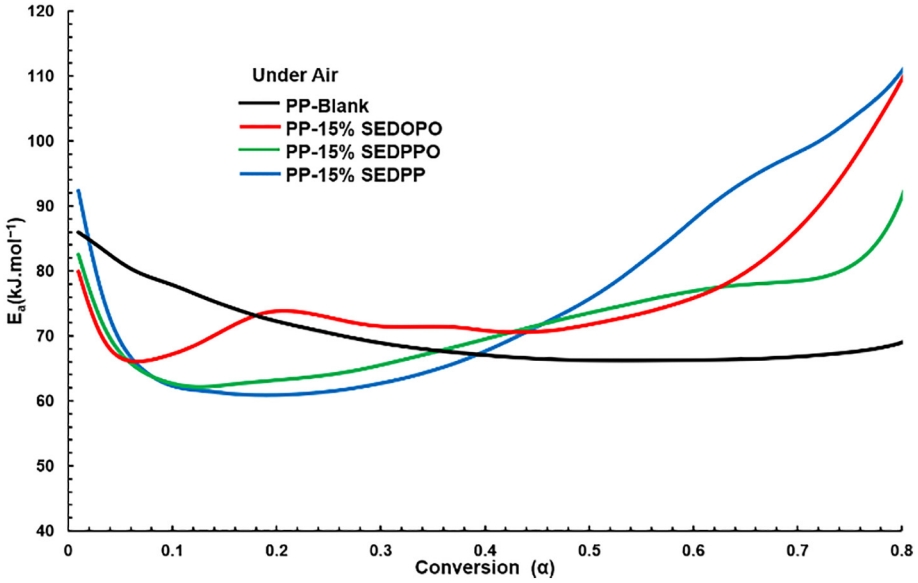

Fig. 4. Variation in activation energy with the degree of conversion for PP blank and PP-FR blends calculated using the Kissinger method.

peroxide radicals, protect the PP polymer chain from fire, and delay the thermal-oxidative degradation (Scheme S1).

3.7. TGA-FTIR analysis of evolved gases

To further understand the thermal decomposition behavior of PP formulations and postulate a mode of action of the bridged sulfone compounds, evolved gases formed during pyrolysis experiments in TGA were analyzed with TGA-FTIR. The 3D plot of the TGA-FTIR spectra for the blank PP and PP-FR blends are shown in Fig. S11 and the extracted FTIR curves of evolved volatiles under different temperatures are presented in Fig. S12. It can be seen in Fig. 5 that the maximum absorbance intensities of all selected pyrolysis products of blank PP and FR-PP blends appear close to the decomposition temperature of the polymer matrix. The release of flammable volatiles like alkanes and alkenes is much lower for sulfone bridged/PP matrix, as shown in Fig. 5. Among PP-FR blends, PP-SEDOPO possesses the lowest flammable volatility, followed by the PP-SEDPPO blend. Thus, a reduced amount of flammable species can lower the fuel response from underlying material and improve the fire resistance of PP.

3.8. DIP-MS and mode of action

There is a limited char formation for the FR-PP blends under N_2 and oxidative conditions compared to the blank PP (Table 5). Bridged sulfone compounds may be active in the gas phase; hence, DIP-MS analysis was performed to evaluate the chemistry of volatiles produced during the thermal decomposition of the FR-PP blends. Fig. S13 shows the total ion chromatogram (TIC) for blank PP and FR-PP blends. SEDPP and SEDPPO blends show the presence of volatile components earlier compared to the blank PP and SEDOPO-blend. Extracted MS- TIC curves of the bridged sulfone-PP blends are presented in Fig. S14, S15, and S16 in the SI part.

The decomposition mechanisms for SEDOPO, SEDPPO, and SEDPP generally involve elimination and hydrolysis reactions. From the evolved gas analysis by TGA-FTIR and DIP-MS measurements, a simplified decomposition pathway for the FR additives is proposed in Scheme 2. For the PP-SEDOPO blend, species corresponding to *m/z* 168, 216, 243, and 335 were observed, representing dibenzofuran, DOPO, ethyl DOPO and methylsulfonyl-ethyl DOPO, respectively (Fig. S14). Initially, the decomposition of SEDOPO leads to the formation of fragments a and b (Scheme 2) and subsequently, the decomposition of DOPO further leads to the formation of stable intermediates such as dibenzofuran

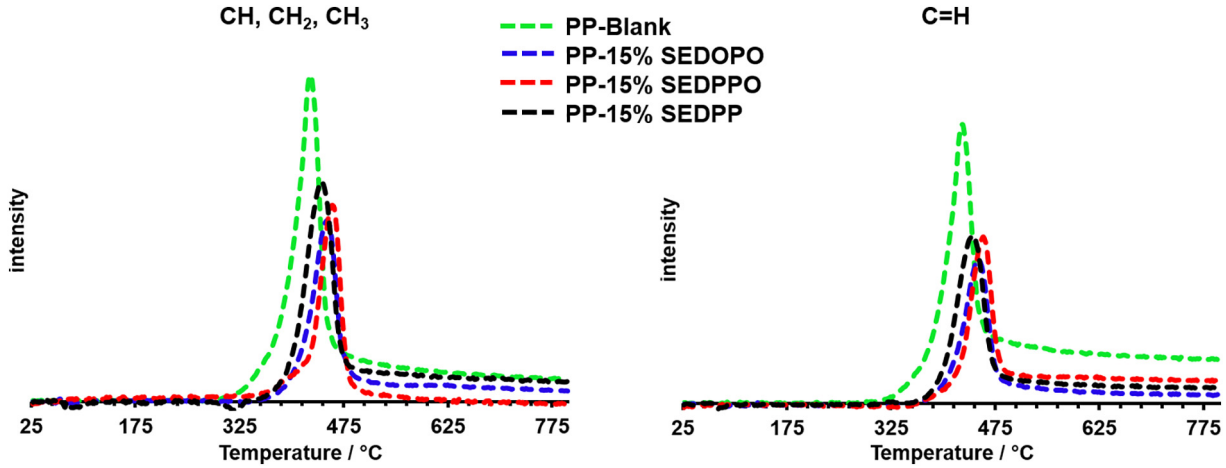

Fig. 5. TGA-FTIR spectra of the total pyrolysis products and intensity of characteristic peaks for selected pyrolysis products of PP blank, PP-15%SEDOPO, SEDPPO, SEDPP blends.

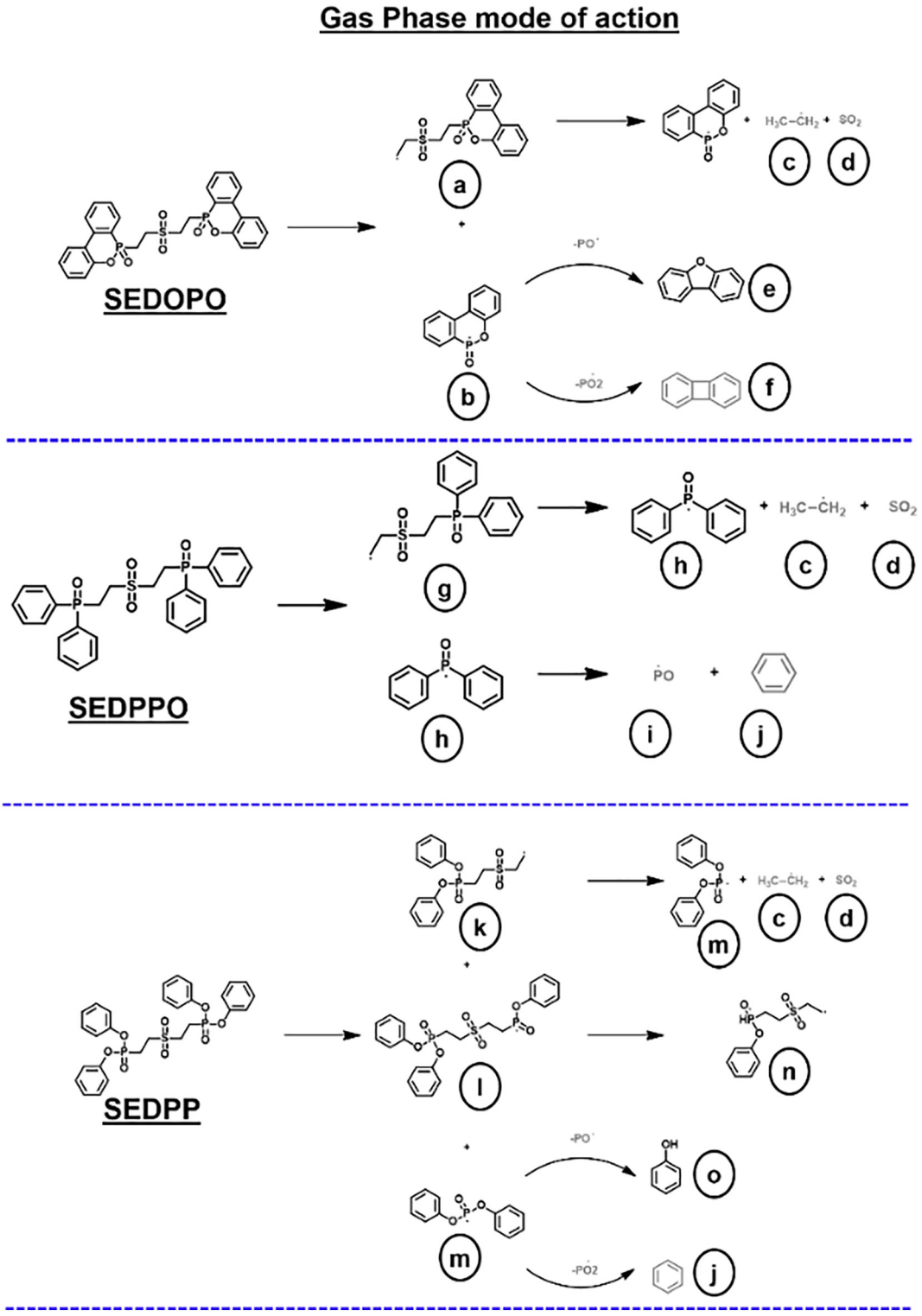

Scheme 2. Proposed thermal decomposition pathways for FRs additives based on DIP-MS analysis. Note: Structures depicted in grey are unidentified species in DIP-MS.

(e) and biphenyl (f) along with the production of $PO^{\bullet}$ and $PO_2^{\bullet}$ active species. Further decomposition of the ethylsulfonyl-ethyl DOPO (a) releases the sulfone containing alkane, which further undergoes C—S bond cleavage and subsequent elimination of alkyl radicals (c) and SO_2 (d). Similarly, for SEDPPO blends, the identified fragments in DIP-MS are summarized in Fig. S15. The PP-SEDPPO thermal decompositions initially provide species such as (2-(ethylsulfonyl)ethyl) diphenylphosphine oxide (g) and diphenylphosphine oxide (h) and compound h undergoes subsequent cleavage to produce active $PO^{\bullet}$ and benzene. The (2-(ethylsulfonyl)ethyl)diphenylphosphine oxide (g) further leads to the elimination of alkyl radicals (c) and sulfone (d), scheme 2. In case of SEDPP blends, cis-elimination leads to the production of diphenyl (2-(ethylsulfonyl)ethyl)phosphonate (k), (2-((2-(oxo(phenoxy)-l4-phosphaneyl)ethyl)sulfonyl)ethyl)phosphonate (l) along with diphenyl phosphonate (m) products. The compound l further decomposes to species n and diphenyl phosphonate

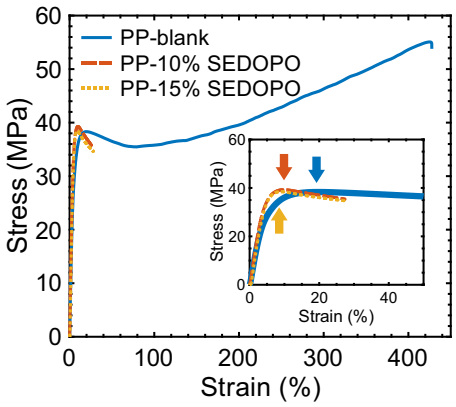

Fig. 6. Stress-strain curves of the PP blank and PP-SEDOPO films of optimized blends. The arrows in the inset plot indicate the yield points.

decomposes to form phenol (o) and benzene (j), as shown in Scheme 2. The decomposition of SO_2 containing compounds is already known in the literature and the proposed scheme is in good agreement with the published data [57]. Based on these observations, a simplistic decomposition pathway for the bridged sulfone compounds and their possible mode of action is proposed in Scheme 2. As highlighted, the production of $PO^{\bullet}$ and SO_2 species for the alkyl sulfone bridged phosphorus FRs boosts their flame inhibition action.

Combining accumulated data acquired from TGA, MCC, and vertical fire test (BKZ-VB), a predominant gas-phase activity for all bridged compounds is thus predicted. Generally, an FR additive should decompose and evolve active species in the gas phase at a temperature close to the polymer matrix decomposition temperature.

3.9. Mechanical behavior for PP films of optimized blends

Melt extrusion of thin films requires high stability of the additives in a molten state and provides samples with partially oriented chains for mechanical tensile testing. As proof of concept, we extruded films from PP-SEDOPO blends, which showed to be the most promising compounds. Fig. 6 shows the exemplary load-strain curves of the films. The curve of the blank PP depicts a shape that is typical for a partially oriented PP film. A yield point indicates the expected transition from elastic to plastic deformation. Since deformation is irreversible after passing the yield point, the latter represents maximum elastic deformation (yield strain) and respective (yield) stress, described in Table 6.

To assess the additive influence on the elastic deformation of PP film, yield stress and yield strain are compared (Table 6). Field stress slightly increased when FR was added, while yield strain was considerably reduced, indicating increased stiffness. On addition of SEDOPO to PP (10 and 15%), the plastic deformation of PP film is hindered as fillers can constrain polymer chain mobility [67]. As a result, the film breaks after having passed the yield point, which means that the extruded film ductility is strongly afflicted by FR addition. Similar effects are also reported for other DOPO derivatives in mechanical flexibility tests [68].

Table 6
Tensile tests result of PP blank and PP-10, 15% SEDOPO films.

Sample Type	Sample name	Nominal melt-pump through-put [cm^3/min]	Yield stress [MPa]	Yield strain [%]
Films	PP-Blank	33.6	34.9 ± 2.0	18.4 ± 3.4
	PP-10% SEDOPO	33.6	38.2 ± 0.9	11.5 ± 1.1
	PP-15% SEDOPO	33.6	36.6 ± 1.9	9.8 ± 1.0

4. Conclusions

In this study, a simplified synthesis procedure for three new alkyl sulfone bridged phosphorus compounds was developed, which has the potential to be upscaled in industry. The bridged sulfone compounds were incorporated in the PP matrix via the melt extrusion process and formed into plates and films. The rheological measurements of the FR/PP blends show that a higher viscosity was achieved for the blends; hence, the degradation mechanism during processing becomes less severe with the bridged sulfone compounds. Fire test results of the PP blends at 10% (around 1% phosphorus content) FR indicated that SEDOPO and SEDPPO have superior flame retardant (FR) performance compared to SEDPP. MCC measurements and cone calorimetry measurements demonstrated the flame retardant effectiveness of PP-SEDPPO and PP-SEDOPO blends as lower heat release rates were observed. Among all PP blends, the lowest peak heat release of 27% and 49% (reduction compared to blank PP) in MCC and cone calorimetry experiments were noted for the 15% PP-SEDOPO blend. The thermal decomposition kinetics experiments respectively were performed and the bridged sulfone derivatives show higher activation energy for the decomposition compared to the blank PP at higher conversion, thus further confirming the stabilizing effect of the bridged sulfone compounds under oxidative conditions. The TGA-FTIR and DIP-MS analysis confirmed that the alkyl sulfone bridged phosphorus derivatives are primarily active in the gas phase via SO_2 and PO species formation. To expand the scope of application of such bridged sulfone compounds, fiber spinning trials and detailed mechanical analysis are planned in future work. In particular, the reduction of FR content with the addition of a suitable synergist will be explored to reduce the adverse effect of high filler loadings on mechanical performance. Future experiments will also address the improvement of dispersion of bridged sulfone derivatives in PP matrix by use of suitable compatibilizers.

Author contribution statements

Rashid Nazir: conceived, planned and carried out the experiments and took the lead in writing the manuscript.

Ali Gooneie: contributed to carry out the Rheology experiments.

Sandro Lehner: contributed to carry out the experiments.

Milijana Jovic: contributed to carry out the experiments.

Patrick Rupper: contributed to carry out the energy dispersive X-ray (EDX) analysis.

Noemie Ott: contributed to carry out the energy dispersive X-ray (EDX) analysis.

Rudolf Hufenus: provide useful feedback and mechanical tests.

Sabyasachi Gaan: conceived and planned the experiments and provided critical feedback and helped shape the research, analysis and writing the manuscript.

Supplementary data to this article can be found online at https://doi.org/10.1016/j.matdes.2021.109459.

Declaration of Competing Interest

The authors declare no conflict of interest.

Acknowledgments

The NMR hardware was partially granted by the Swiss National Science Foundation (SNSF, Grant 206021_150638/1). We thank Mr. Mathias Lienhard for compounding and extrusion trials and Mr. Markus Hilber for tensile testing. We would also like to thank Ms. Ayesha Nadeem for diligent proofreading of the manuscript.

References

[1] S.A. Arvidson, K.C. Wong, R.E. Gorga, S.A. Khan, Structure, molecular orientation, and resultant mechanical properties in core/ sheath poly(lactic acid)/polypropylene composites, Polymer 53 (3) (2012) 791–800.

[2] H. Palza, R. Vergara, P. Zapata, Composites of polypropylene melt blended with synthesized silica nanoparticles, Compos. Sci. Technol. 71 (4) (2011) 535–540.

[3] R. Nazir, S. Gaan, Recent developments in P(O/S)–N containing flame retardants, J. Appl. Polym. Sci. 137 (1) (2020) 47910.

[4] B. Li, M. Xu, Effect of a novel charring–foaming agent on flame retardancy and thermal degradation of intumescent flame retardant polypropylene, Polym. Degrad. Stab. 91 (6) (2006) 1380–1386.

[5] A.F. Grand, Effect of experimental conditions on the evolution of combustion products using a modified University of Pittsburgh Toxicity Test Apparatus, Journal of Fire Sciences 3 (4) (1985) 280–304.

[6] M.M. Hirschler, Fire Hazard and toxic potency of the smoke from burning materials, Journal of Fire Sciences 5 (5) (1987) 289–307.

[7] R. Nazir, D. Parida, J. Borgstädt, S. Lehner, M. Jovic, D. Rentsch, E. Bülbül, A. Huch, S. Altenried, Q. Ren, P. Rupper, S. Annaheim, S. Gaan, In-situ phosphine oxide physical networks: a facile strategy to achieve durable flame retardant and antimicrobial treatments of cellulose, Chem. Eng. J. 128028 (2020).

[8] S. Zhang, A.R. Horrocks, A review of flame retardant polypropylene fibres, Prog. Polym. Sci. 28 (11) (2003) 1517–1538.

[9] J. Wang, L. Wang, A. Xiao, Recent research Progress on the flame-retardant mechanism of halogen-free flame retardant polypropylene, Polym.-Plast. Technol. Eng. 48 (3) (2009) 297–302.

[10] P.J. Gale, Mass spectrometric studies of the reactivity of antimony trioxide with halogenated flame retardants in the pyrolysis of plastics, Int. J. Mass Spectrom. Ion Process. 100 (1990) 313–322.

[11] M. Alaee, P. Arias, A. Sjödin, Å. Bergman, An overview of commercially used brominated flame retardants, their applications, their use patterns in different countries/regions and possible modes of release, Environ. Int. 29 (6) (2003) 683–689.

[12] Z.-Y. Wang, Y. Liu, Q. Wang, Flame retardant polyoxymethylene with aluminium hydroxide/melamine/novolac resin synergistic system, Polym. Degrad. Stab. 95 (6) (2010) 945–954.

[13] A.A. Sener, E. Demirhan, The investigation of using magnesium hydroxide as a flame retardant in the cable insulation material by cross-linked polyethylene, Mater. Des. 29 (7) (2008) 1376–1379.

[14] T. Xu, X. Huang, Y. Zhao, Investigation into the properties of asphalt mixtures containing magnesium hydroxide flame retardant, Fire Saf. J. 46 (6) (2011) 330–334.

[15] A.U.R. Shah, D.W. Lee, Y.Q. Wang, A. Wasy, K.C. Ham, K. Jayaraman, B.-S. Kim, J.-I. Song, Effect of concentration of ATH on mechanical properties of polypropylene/aluminium trihydrate (PP/ATH) composite, Trans. Nonferrous Metals Soc. China 24 (2014) s81–s89.

[16] R.C. Nicolas, C.-E. Wilén, M. Roth, R. Pfaendner, R.E. King III, Azoalkanes: a novel class of flame retardants, Macromol. Rapid Commun. 27 (12) (2006) 976–981.

[17] M. Aubert, M. Roth, R. Pfaendner, C.-E. Wilén, Azoalkanes: a novel class of additives for cross-linking and controlled degradation of Polyolefins, Macromol. Mater. Eng. 292 (6) (2007) 707–714.

[18] M. Aubert, C.-E. Wilén, R. Pfaendner, S. Kniesel, H. Hoppe, M. Roth, Bis(1-propyloxy-2,2,6,6-tetramethylpiperidin-4-yl)-diazene – an innovative multifunctional radical generator providing flame retardancy to polypropylene even after extended artificial weathering, Polym. Degrad. Stab. 96 (3) (2011) 328–333.

[19] D.C.O. Marney, L.J. Russell, T.M. Stark, The influence of an N-alkoxy HALS on the decomposition of a brominated fire retardant in polypropylene, Polym. Degrad. Stab. 93 (3) (2008) 714–722.

[20] K. Cao, S.-l. Wu, S.-l. Qiu, Y. Li, Z. Yao, Synthesis of N-Alkoxy hindered amine containing Silane as a multifunctional flame retardant synergist and its application in intumescent flame retardant polypropylene, Ind. Eng. Chem. Res. 52 (1) (2013) 309–317.

[21] R. Pfaendner, How will additives shape the future of plastics? Polym. Degrad. Stab. 91 (9) (2006) 2249–2256.

[22] R. Pfaendner, Nitroxyl radicals and nitroxylethers beyond stabilization: radical generators for efficient polymer modification, Comptes Rendus Chimie 9 (11) (2006) 1338–1344.

[23] S.M.A. Douglas Wayne Horsey, Leonard Harris Davis, Robert Leo Gray Darrell David Dyas Jr., Anunay Gupta, Bruce Vincent Hein, Joseph Stephen Puglisi, Ramanathan Ravichandran, Paul Shields, Rangarajan Srinivasan, Hindered amine flame retardant compositions, 1999.

[24] M. Roth, Flame retardant compositions comprising sterically hindered amines, 2009.

[25] D.A. Abdel-Ilah Basbas, Robert Cordova, Michael Peter Difazio, Walter Fischer, Joseph A. Kotrola, Tiziano Nocentini, James Robbins, Kai-Uwe Schöning, Process for the preparation of sterically hindered nitroxyl ethers, 2008.

[26] S. Zhang, A.R. Horrocks, R. Hull, B.K. Kandola, Flammability, degradation and structural characterization of fibre-forming polypropylene containing nanoclay–flame retardant combinations, Polym. Degrad. Stab. 91 (4) (2006) 719–725.

[27] S.V. Levchik, E.D. Weil, Overview of recent developments in the flame retardancy of polycarbonates, Polym. Int. 54 (7) (2005) 981–998.

[28] W. Zhao, B. Li, M. Xu, L. Zhang, F. Liu, L. Guan, Synthesis of a novel flame retardant containing phosphorus and sulfur and its application in polycarbonate, Polym. Eng. Sci. 52 (11) (2012) 2327–2335.

[29] C. Luo, J. Zuo, F. Wang, Y. Yuan, F. Lin, H. Huang, J. Zhao, High refractive index and flame retardancy of epoxy thermoset cured by tris (2- mercaptoethyl) phosphate, Polym. Degrad. Stab. 129 (2016) 7–11.

[30] U. Braun, U. Knoll, B. Schartel, T. Hoffmann, D. Pospiech, J. Artner, M. Ciesielski, M. Döring, R. Perez-Graterol, J.K.W. Sandler, V. Altstädt, Novel phosphorus-containing poly(ether sulfone)s and their blends with an epoxy resin: thermal decomposition and fire Retardancy, Macromol. Chem. Phys. 207 (16) (2006) 1501–1514.

[31] J. Wagner, P. Deglmann, S. Fuchs, M. Ciesielski, C.A. Fleckenstein, M. Döring, A flame retardant synergism of organic disulfides and phosphorous compounds, Polym. Degrad. Stab. 129 (2016) 63–76.

[32] W. Pawelec, A. Holappa, T. Tirri, M. Aubert, H. Hoppe, R. Pfaendner, C.-E. Wilén, Disulfides – effective radical generators for flame retardancy of polypropylene, Polym. Degrad. Stab. 110 (2014) 447–456.

[33] A. Ballistreri, G. Montaudo, E. Scamporrino, C. Puglisi, D. Vitalini, S. Cucinella, Intumescent flame retardants for polymers. IV. The polycarbonate–aromatic sulfonates system, J. Polym. Sci. A Polym. Chem. 26 (8) (1988) 2113–2127.

[34] S. Hou, Y.J. Zhang, P. Jiang, Phosphonium sulfonates as flame retardants for polycarbonate, Polym. Degrad. Stab. 130 (2016) 165–172.

[35] A. Nodera, T. Kanai, Thermal decomposition behavior and flame retardancy of polycarbonate containing organic metal salts: effect of salt composition, J. Appl. Polym. Sci. 94 (5) (2004) 2131–2139.

[36] J. Green, Mechanisms for flame Retardancy and smoke suppression - a review, Journal of Fire Sciences 14 (6) (1996) 426–442.

[37] M. Lewin, J. Zhang, E. Pearce, J. Gilman, Flammability of polyamide 6 using the sulfamate system and organo-layered silicate, Polym. Adv. Technol. 18 (9) (2007) 737–745.

[38] M. Lewin, J. Brozek, M.M. Martens, The system polyamide/sulfamate/dipentaerythritol: flame retardancy and chemical reactions, Polym. Adv. Technol. 13 (10−12) (2002) 1091–1102.

[39] M. Lewin, Flame retarding of polymers with Sulfamates. I. Sulfation of cotton and wool, Journal of Fire Sciences 15 (4) (1997) 263–276.

[40] Y. Chen, H. Peng, J. Li, Z. Xia, H. Tan, A novel flame retardant containing phosphorus, nitrogen, and sulfur, J. Therm. Anal. Calorim. 115 (2) (2014) 1639–1649.

[41] J. He, G. Cai, C.A. Wilkie, The effects of several sulfonates on thermal and fire retardant properties of poly(methyl methacrylate) and polystyrene, Polym. Adv. Technol. 25 (2) (2014) 160–167.

[42] C.L. Rasmussen, P. Glarborg, P. Marshall, Mechanisms of radical removal by SO2, Proc. Combust. Inst. 31 (1) (2007) 339–347.

[43] M.R. Zachariah, O.I. Smith, Experimental and numerical studies of sulfur chemistry in H2/O2/SO2 flames, Combustion and Flame 69 (2) (1987) 125–139.

[44] B.A. Howell, Y.G. Daniel, The impact of sulfur oxidation level on flame retardancy, Journal of Fire Sciences 36 (6) (2018) 518–534.

[45] R.A. Stockland, R.I. Taylor, L.E. Thompson, P.B. Patel, Microwave-assisted Regioselective addition of P(O)−H bonds to alkenes without added solvent or catalyst, Org. Lett. 7 (5) (2005) 851–853.

[46] K.A. Salmeia, A. Gooneie, P. Simonetti, R. Nazir, J.-P. Kaiser, A. Rippl, C. Hirsch, S. Lehner, P. Rupper, R. Hufenus, S. Gaan, Comprehensive study on flame retardant polyesters from phosphorus additives, Polym. Degrad. Stab. 155 (2018) 22–34.

[47] S. Vyazovkin, K. Chrissafis, M.L. Di Lorenzo, N. Koga, M. Pijolat, B. Roduit, N. Sbirrazzuoli, J.J. Suñol, ICTAC kinetics committee recommendations for collecting experimental thermal analysis data for kinetic computations, Thermochim. Acta 590 (2014) 1–23.

[48] Y. Saga, D. Han, S.-i. Kawaguchi, A. Ogawa, L.-B. Han, A salt-free synthesis of 1,2-bisphosphorylethanes via an efficient PMe3-catalyzed addition of >P(O)H to vinylphosphoryl compounds, Tetrahedron Lett. 56 (38) (2015) 5303–5305.

[49] T. Hirai, L.-B. Han, Air-induced anti-Markovnikov addition of secondary phosphine oxides and H-Phosphinates to alkenes, Org. Lett. 9 (1) (2007) 53–55.

[50] L.L. Khemchyan, J.V. Ivanova, S.S. Zalesskiy, V.P. Ananikov, I.P. Beletskaya, Z.A. Starikova, Unprecedented control of selectivity in nickel-catalyzed Hydrophosphorylation of alkynes: efficient route to mono- and bisphosphonates, Adv. Synth. Catal. 356 (4) (2014) 771–780.

[51] L.-B. Han, C.-Q. Zhao, Stereospecific addition of H−P bond to alkenes: a simple method for the preparation of (RP)-Phenylphosphinates, The Journal of Organic Chemistry 70 (24) (2005) 10121–10123.

[52] Y. Lin, D. Bernardi, E. Doris, F. Taran, Phosphine-catalyzed synthesis of unsymmetrical 1,3-Bis- and Trisphosphorus ligands, Synlett 2009 (09) (2009) 1466–1470.

[53] A. Gooneie, P. Simonetti, K.A. Salmeia, S. Gaan, R. Hufenus, M.P. Heuberger, Enhanced PET processing with organophosphorus additive: flame retardant products with added-value for recycling, Polym. Degrad. Stab. 160 (2019) 218–228.

[54] P. Simonetti, R. Nazir, A. Gooneie, S. Lehner, M. Jovic, K.A. Salmeia, R. Hufenus, A. Rippl, J.-P. Kaiser, C. Hirsch, B. Rubi, S. Gaan, Michael addition in reactive extrusion: a facile sustainable route to developing phosphorus based flame retardant materials, Compos. Part B 178 (2019) 107470.

[55] S. Liang, M. Neisius, H. Mispreuve, R. Naescher, S. Gaan, Flame retardancy and thermal decomposition of flexible polyurethane foams: structural influence of organophosphorus compounds, Polym. Degrad. Stab. 97 (11) (2012) 2428–2440.

[56] M.E. Üreyen, E. Kaynak, G. Yüksel, Flame-retardant effects of cyclic phosphonate with HALS and fumed silica in polypropylene, J. Appl. Polym. Sci. 137 (4) (2020) 48308.

[57] A. Battig, J.C. Markwart, F.R. Wurm, B. Schartel, Sulfur's role in the flame retardancy of thio-ether–linked hyperbranched polyphosphoesters in epoxy resins, Eur. Polym. J. 122 (2020) 109390.

[58] J.A.P. Solorzano, K.A.M. Moinuddin, S. Tretsiakova-McNally, P. Joseph, A study of the thermal degradation and combustion characteristics of some materials commonly used in the construction sector, Polymers (Basel) 11 (11) (2019).

[59] A. Przystas, M. Jovic, K.A. Salmeia, D. Rentsch, L. Ferry, H. Mispreuve, H. Perler, S. Gaan, Some key factors influencing the flame Retardancy of EDA-DOPO containing flexible polyurethane foams, Polymers 10 (10) (2018).

[60] A. Buczko, T. Stelzig, L. Bommer, D. Rentsch, M. Heneczkowski, S. Gaan, Bridged DOPO derivatives as flame retardants for PA6, Polym. Degrad. Stab. 107 (2014) 158–165.

[61] I. Butnaru, P.M. Fernández-Ronco, J. Czech-Polak, M. Heneczkowski, M. Bruma, S. Gaan, Effect of Meltable Triazine-DOPO additive on rheological, mechanical, and flammability properties of PA6, Polymers 7 (8) (2015).
[62] Q. Dong, Y. Ding, B. Wen, F. Wang, H. Dong, S. Zhang, T. Wang, M. Yang, Improvement of thermal stability of polypropylene using DOPO-immobilized silica nanoparticles, Colloid Polym. Sci. 290 (14) (2012) 1371–1380.
[63] A.C. Kolbert, J.G. Didier, L. Xu, Mechanochemical degradation of ethylene—propylene copolymers: characterization of olefin chain ends, Macromolecules 29 (27) (1996) 8591–8598.
[64] D.M. Mowery, R.L. Clough, R.A. Assink, Identification of oxidation products in selectively labeled polypropylene with solid-state 13C NMR techniques, Macromolecules 40 (10) (2007) 3615–3623.
[65] H. Hinsken, S. Moss, J.-R. Pauquet, H. Zweifel, Degradation of polyolefins during melt processing, Polym. Degrad. Stab. 34 (1) (1991) 279–293.
[66] A.V. Tobolsky, P.M. Norling, N.H. Frick, H. Yu, On the mechanism of autoxidation of three vinyl polymers: polypropylene, ethylene-propylene rubber, and poly(ethyl acrylate), J. Am. Chem. Soc. 86 (19) (1964) 3925–3930.
[67] A. Gooneie, R. Hufenus, Hybrid carbon nanoparticles in polymer matrix for efficient connected networks: self-assembly and continuous pathways, Macromolecules 51 (10) (2018) 3547–3562.
[68] A. Gooneie, P. Simonetti, P. Rupper, R. Nazir, M. Jovic, S. Gaan, M.P. Heuberger, R. Hufenus, Stabilizing effects of novel phosphorus flame retardant on PET for high-temperature applications, Mater. Lett. 276 (2020) 128225.